Magic-angle spinning 13C NMR spectroscopy of transition-metal carbonyl clusters

ARTICLE *in* THE JOURNAL OF PHYSICAL CHEMISTRY · FEBRUARY 1989

Impact Factor: 2.78 · DOI: 10.1021/j100341a029

Magic-Angle Spinning ^{13}C NMR Spectroscopy of Transition-Metal Carbonyl Clusters

Thomas H. Walter,† Linda Reven, and Eric Oldfield*

School of Chemical Sciences, University of Illinois at Urbana-Champaign, Urbana, Illinois 61801
(Received: July 12, 1988)

A variety of ^{13}C-enriched metal carbonyl clusters ($Fe_3(CO)_{12}$, $Ru_3(CO)_{12}$, $Os_3(CO)_{12}$, $Rh_6(CO)_{16}$, and $Ir_4(CO)_{12}$) have been examined by magic-angle spinning ^{13}C nuclear magnetic resonance spectroscopy. The results yield both the isotropic chemical shifts and the principal components of the chemical shift tensor for each crystallographically distinct carbonyl site, as well as their spin-lattice relaxation times. With the 0.25-ppm resolution obtained at high field (8.45 T), effects from ^{13}C-^{13}C and ^{13}C-^{103}Rh J coupling, as well as incompletely averaged ^{13}C-$^{191}Ir/^{193}Ir$ dipolar coupling, can be discerned. The chemical shift tensor components, obtained from analysis of spinning sideband intensities, are shown to be in generally good agreement with values previously obtained from broad-line spectra. The motionally averaged chemical shift tensor components for $Fe_3(CO)_{12}$, which is fluxional at room temperature, are shown to be consistent with a previously proposed exchange process.

Metal carbonyl clusters, organometallic complexes containing two or more metal atoms surrounded by carbonyl ligands, have been widely investigated both as homogeneous catalysts[1] and as models for supported metal crystallite catalysts.[2] As part of a program to investigate the structures and mobilities of metal carbonyl clusters supported on metal oxides using ^{13}C magic-angle spinning (MAS) nuclear magnetic resonance (NMR) spectroscopy,[3] we have examined a number of clusters in the crystalline solid state. There have been relatively few ^{13}C MAS NMR studies of rigid metal carbonyl clusters,[4,5] although several fluxional clusters have been examined by Hanson and co-workers.[6-10] A number of metal carbonyl complexes have also been examined by using broad-line techniques,[11] providing information on the chemical shift anisotropy (CSA) of the carbonyl ligand. Carbonyl chemical shifts are found to be highly anisotropic, with anisotropy parameters of typically 350-450 ppm for terminal carbonyls.[11] These large chemical shift anisotropies provide a sensitive probe for investigating motion of the carbonyl ligand both in the crystalline solid state[12] and in complexes supported on metal oxides.[13] Unfortunately, broad-line NMR techniques can provide only limited information on metal carbonyl clusters, because of the severe overlap between resonances from each distinct carbonyl site. One method of obtaining high-resolution spectra without completely eliminating the CSA information is to perform slow MAS experiments, in which the spinning speed is small relative to the anisotropy. As first shown by Lippmaa et al.[14] and Stejskal et al.,[15] such slow-spinning experiments yield spectra in which a series of spinning sidebands flank the centerband resonance (located at the isotropic chemical shift), with a separation equal to the spinning frequency. The relative intensities of the sidebands can be analyzed[16,17] to obtain the principal components of the chemical shift tensor. We demonstrate in this article that slow-spinning MAS experiments can be used to obtain the principal components of the shielding tensors for all sites in a variety of metal carbonyl clusters. The CSA parameters we obtain are in generally good agreement with the earlier broad-line results. However, the new results allow in addition the observation of both crystallographic inequivalence and J-coupling effects. The chemical shift anisotropy parameters obtained from these experiments can be used to provide information on fluxionality in the solid state, as demonstrated for $Fe_3(CO)_{12}$.

Experimental Section

Chemical Aspects. All metal carbonyl complexes were obtained from Strem Chemicals (Newburyport, MA), with the exception of $Fe_3(CO)_{12}$, which was obtained from Aldrich (Milwaukee, WI). Samples were enriched in ^{13}C by exchange with 99% ^{13}CO (Monsanto Research Corporation; Miamisburg, OH). For $Os_3(CO)_{12}$, $Rh_6(CO)_{16}$, and $Ir_4(CO)_{12}$, which are all relatively insoluble and stable to at least 200 °C,[18] exchange was carried out in decahydronaphthalene at 150 °C for 24-48 h. In each case, the crude product was purified by recrystallization. The same procedure was found to cause decomposition of $Fe_3(CO)_{12}$ and $Ru_3(CO)_{12}$. Thus for $Fe_3(CO)_{12}$, exchange was carried out in heptane at room temperature for 6 days, and the product was purified by recrystallization from warm toluene. $Ru_3(CO)_{12}$ was dissolved in heptane and exchange was carried out at 80 °C for 8 h, the product being recrystallized from dichloroethane. With the exception of $Ir_4(CO)_{12}$, which is insoluble at room temperature, each sample was examined by solution ^{13}C NMR to verify both purity and uniformity of enrichment. Overall enrichment levels were determined by electron impact mass spectrometry.

NMR Spectroscopy. ^{13}C NMR spectra were obtained on Fourier transform NMR spectrometers operating at 37.8, 90.5, and 125.7 MHz, using home-built spectrometers that have been described previously.[19,20] Magic-angle spinning spectra at all field strengths were obtained by using home-built probes employing spinners of the Andrew-Beams type, with 10-mm o.d. (3.2-kHz maximum spinning speed) or 7-mm o.d. (5.5-kHz maximum spinning speed) rotors made of delrin. Some 90-MHz spectra were also obtained by using a Doty (Doty Scientific; Columbia, SC) probe. All spectra were obtained with 90° pulse excitation (typically 5-10 μs). The magic angle was set by observing the ^{79}Br resonance from KBr,[21] added to each sample. Exponential

† Present address: Millipore, Waters Chromatography Division, 34 Maple St., Milford, MA 01757.

(1) Muetterties, E. L.; Krause, M. J. *Angew. Chem., Int. Ed. Engl.* **1983**, *22*, 135.
(2) Muetterties, E. L.; Rhodin, T. N.; Band, E.; Brucker, C. F.; Pretzer, W. R. *Chem. Rev.* **1979**, *79*, 91.
(3) Walter, T. H.; Frauenhoff, G. R.; Shapley, J. R.; Oldfield, E. *Inorg. Chem.* **1988**, *27*, 2561.
(4) Hasselbring, L.; Lamb, H.; Dybowski, C.; Gates, B.; Rheingold, A. *Inorg. Chim. Acta* **1987**, *127*, L49.
(5) Dorn, H. C.; Hanson, B E.; Motell, E. *J. Organomet. Chem.* **1982**, *224*, 181.
(6) Hanson, B. E. In *Advances in Dynamic Stereochemistry*; Gielin, M. F., Ed.; Freund: London, 1985; p 53.
(7) Dorn, H.; Hanson, B. E.; Motell, E. *Inorg. Chim. Acta* **1981**, *54*, L71.
(8) Hanson, B. E.; Sullivan, M. J.; Davis, R. J. *J. Am. Chem. Soc.* **1984**, *106*, 251.
(9) Hanson, B. E.; Lisic, E. C.; Petty, J. T.; Iannaconne, G. A. *Inorg. Chem.* **1986**, *25*, 4062.
(10) Hanson, B. E.; Lisic, E. C. *Inorg. Chem.* **1986**, *25*, 716.
(11) Gleeson, J. W.; Vaughan, R. W. *J. Chem. Phys.* **1983**, *78*, 5384.
(12) Spiess, H. W.; Grosescu, R.; Haeberlen, U. *Chem. Phys.* **1974**, *6*, 226.
(13) Walter, T. H.; Thompson, A.; Keniry, M.; Shinoda, S.; Brown, T. L.; Gutowsky, H. S.; Oldfield, E. *J. Am. Chem. Soc.* **1988**, *110*, 1065.
(14) Lippmaa, E.; Alla, M.; Tuhern, T. *Proc. Congr. Ampere, 19th, 1976* **1976**, 113.
(15) Stejskal, E. O.; Schaefer, J.; McKay, R. A. *J. Magn. Reson.* **1977**, *25*, 569.
(16) Maricq, M. M.; Waugh, J. S. *J. Chem. Phys.* **1979**, *70*, 3300.
(17) Herzfeld, J.; Berger, A. E. *J. Chem. Phys.* **1980**, *73*, 6021.
(18) Calderazzo, F.; Ercoli, R.; Natta, G. In *Organic Syntheses via Metal Carbonyls*; Wender, I., Ed.; Interscience: New York, 1968; p 39.
(19) Oldfield, E.; Meadows, M. *J. Magn. Reson.* **1978**, *31*, 327.
(20) Smith, K. A.; Kirkpatrick, R. J.; Oldfield, E.; Henderson, D. M. *Am. Mineral.* **1983**, *68*, 1206.
(21) Frye, J. S.; Maciel, G. E. *J. Magn. Reson.* **1982**, *48*, 125.

0022-3654/89/2093-1320$01.50/0

TABLE I: Carbon-13 Isotropic Chemical Shifts for Some Solid Metal Carbonyl Clusters

compound	site	δ_i(solution),[a] ppm	δ_i(solid),[a,b] ppm
$Os_3(CO)_{12}$	axial	182.3 (1)[c]	187.3 (1), 186.1 (1), 184.4 (2), 183.9 (1), 181.0 (1)
	equatorial	170.4 (1)[c]	173.7 (1), 173.3 (1), 172.1 (1), 171.1 (1), 170.0 (1), 167.9 (1)
$Ru_3(CO)_{12}$	axial		212.3 (1), 211.0 (1), 209.6 (2), 208.7 (1), 206.4 (1)
	equatorial	199.7 (1)[c,d]	191.6 (1), 191.2 (1), 189.4 (2), 187.9 (1), 186.1 (1)
$Rh_6(CO)_{16}$	terminal	180.1 (3)[e]	179.4 (1), 180.1 (1), 181.2 (3), 182.4 (1)
	bridging	231.5 (1)[e]	229.9 (1), 234.1 (1)
$Ir_4(CO)_{12}$		154.2[f]	156
$Fe_3(CO)_{12}$		212.9[c,d]	225.5 (1), 223.8 (1), 213.5 (1), 209.7 (1), 202.9 (1), 201.4 (1)

[a] Numbers in parentheses indicate relative intensities. [b] Estimated uncertainty ±0.5 ppm. [c] Reference 24. [d] Exchange-averaged. [e] Reference 30. [f] Reference 32.

apodization (10 Hz) was applied to the free induction decays for sensitivity enhancement, and the digital resolution was typically 2 Hz/point. Spin–lattice relaxation times were measured by using the saturating comb saturation-recovery method, rather than by inversion-recovery, to avoid the necessity of waiting for complete relaxation between repetitions.[22] Chemical shifts are reported in ppm from TMS with adamantane as an external chemical shift reference, the methine resonance being assigned a chemical shift of 29.50 ppm.[23] The principal components of the chemical shift tensor, δ_{11}, δ_{22}, and δ_{33}, were obtained from spinning sideband intensities by using the graphical method of Herzfeld and Berger.[17] The isotropic chemical shift, δ_i, the shielding anisotropy, $\Delta\delta$, and the asymmetry parameter, η, are defined by

$$\delta_i = \tfrac{1}{3}(\delta_{11} + \delta_{22} + \delta_{33})$$

$$\Delta\delta = \delta_{33} - \tfrac{1}{2}(\delta_{11} + \delta_{22})$$

$$\eta = \frac{\delta_{22} - \delta_{11}}{\delta_{33} - \delta_i}$$

where we have used the convention that $|\delta_{33} - \delta_i| \geq |\delta_{11} - \delta_i| \geq |\delta_{22} - \delta_i|$.

Results and Discussion

$Os_3(CO)_{12}$. We show in Figure 1A the ^{13}C MAS NMR spectrum obtained for 60% ^{13}C-enriched $Os_3(CO)_{12}$ at 38 MHz. At this field strength, the 350-ppm chemical shift anisotropy of the carbonyl ligands results in a spectrum that extends over a range of 15 kHz. Thus, when spinning at 3 kHz, six sets of spinning sidebands are obtained. The centerband resonances, which are located by changing the spinning speed and identifying the peaks whose positions are invariant, are indicated. Two distinct centerband resonances are observed, arising from the two carbonyl environments in this cluster: equatorial carbonyls, which lie in the Os_3 plane, and axial carbonyls, which are normal to it. Despite the 12-ppm separation between these resonances, they were not resolved in previous broad-line spectra.[11] As shown in Figure 1B, closer inspection of the centerband resonances reveals a large amount of fine structure, as previously noted,[4] which arises from the effects of symmetry lowering in the solid state. While $Os_3(CO)_{12}$ possesses D_{3h} point symmetry in solution,[24,25] it crystallizes in a monoclinic lattice containing $Os_3(CO)_{12}$ units devoid of symmetry.[26] Thus, although all six axial carbonyls and all six equatorial carbonyls are equivalent in solution, they are inequivalent in the solid state, so that a maximum of 12 resonances may be observed. While not all of these sites can be clearly resolved at 38 MHz (see Figure 1B), we find a dramatic improvement in resolution at 90 MHz, as shown in Figure 1C, allowing 10 of the 12 resonances to be resolved. The isotropic chemical shifts for all peaks are listed in Table I. Our values are in general agreement with those of Hasselbring et al.,[4] although they are uniformly more shielded by approximately 0.5 ppm.

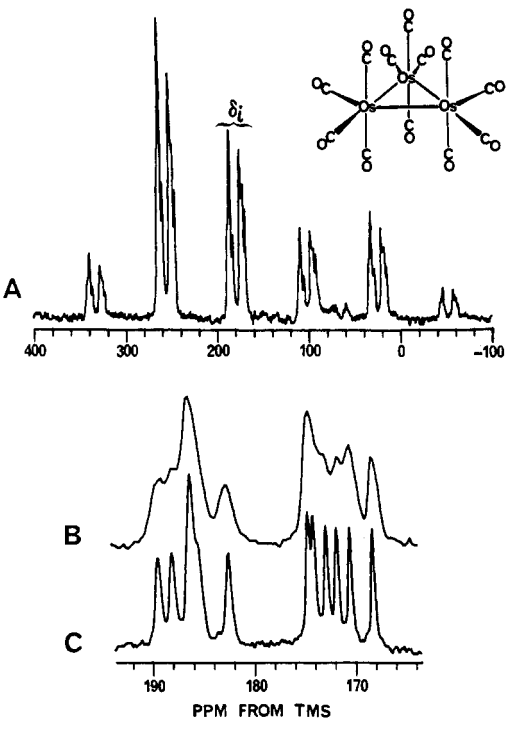

Figure 1. Carbon-13 MAS NMR spectra of $[^{13}C]Os_3(CO)_{12}$. (A) Spectrum obtained at 38 MHz; 3.0-kHz spinning speed, 80 acquisitions with a 500-s recycle delay. (B) Expanded view showing centerband fine structure. (C) Expanded view of centerband resonances from a spectrum obtained at 90 MHz; 2.8-kHz spinning speed, 80 acquisitions with a 500-s recycle delay.

An interesting effect evident in Figure 1C is the significant difference between the line widths of the axial (high frequency) and equatorial (low frequency) carbonyl resonances, which are 40 and 25 Hz (full width at half-height, fwhh), respectively, at 90 MHz. We attribute this difference to unresolved ^{13}C–^{13}C J coupling. It is known that $^2J_{CC}$ coupling constants for carbonyls that are trans across a metal atom are much larger than those of carbonyls with a cis orientation, with typical values being $^2J_{CC}$(trans) ~ 30–35 Hz[27] and $^2J_{CC}$(cis) ~ 1–5 Hz.[28] Thus for the axial carbonyls, which are all trans to another axial carbonyl, each resonance should consist of a doublet with $^2J_{CC}$ ~ 33 Hz from the 60% of the isotopomers having a ^{13}C in the trans position and a singlet from the 40% having a ^{12}C in the trans position. This coupling cannot be observed in solution, where all the axial carbonyls are equivalent, but is made observable in the solid state by their inequivalence. This observation of $^2J_{CC}$(trans) is the first direct evidence that the high-frequency (downfield) resonance(s) in $Os_3(CO)_{12}$ are indeed due to the axial carbonyls. Although it has been observed for derivatives of $Os_3(CO)_{12}$ that an axial carbonyl resonates at lower field than an equatorial carbonyl on the same osmium center,[27] there is no information present in the solution spectrum of $Os_3(CO)_{12}$ to allow an assignment of the two resonances.[24,25]

From the relative intensities of the spinning sidebands in the spectrum of Figure 1A, we can obtain the principal components

(22) Fukushima, E.; Roeder, S. B. W. *Experimental Pulse NMR*; Addison-Wesley: Reading, MA, 1981; pp 174–176.
(23) VanderHart, D. L. *J. Chem. Phys.* **1986**, *84*, 1196.
(24) Forster, A.; Johnson, B. F. G.; Lewis, J.; Matheson, T. W.; Robinson, B. H.; Jackson, W. G. *J. Chem. Soc., Chem. Commun.* **1974**, 1042.
(25) Aime, S.; Gambino, O.; Milone, L.; Sappa, E.; Rosenberg, E. *Inorg. Chim. Acta* **1975**, *15*, 53.
(26) Corey, E. R.; Dahl, L. F. *Inorg. Chem.* **1962**, *1*, 521.
(27) Tachikawa, M.; Richter, S. I.; Shapley, J. R. *J. Organomet. Chem.* **1977**, *128*, C9.
(28) Aime, S.; Osella, D. *J. Chem. Soc., Chem. Commun.* **1981**, 300.

TABLE II: Principal Components, Anisotropies, and Asymmetry Parameters of the Carbon-13 Chemical Shift Tensor for Some Metal Carbonyl Clusters

compound	site	δ_i, ppm	δ_{11},[a] ppm	δ_{22},[a] ppm	δ_{33},[a] ppm	$\Delta\delta$,[a] ppm	η
$Os_3(CO)_{12}$	axial	186	313	304	−59	367	0.04
	equatorial	171	289	289	−64	353	0.00
	static[b]	176	292	292	−55	347	0.00
$Ru_3(CO)_{12}$	axial	210	346	338	−54	396	0.03
	equatorial	189	330	312	−74	395	0.07
	static[b]	201	348	319	−63	397	0.11
$Rh_6(CO)_{16}$	terminal	181	320	299	−76	386	0.08
	static[b]	180	315	305	−80	390	0.04
	bridging	230	301	292	97	199	0.07
	static[b]	231	296	296	102	194	0.00
$Ir_4(CO)_{12}$		156	274	274	−81	355	0.00
	static[b]	167	277	277	−53	330	0.00
$Fe_3(CO)_{12}$		203	342	322	−54	386	0.08
		210	344	328	−42	378	0.06
		213	348	311	−20	350	0.16
		225	328	321	26	298	0.04
	static[b]	212	325	316	−6	327	0.04

[a] Estimated uncertainty ±10 ppm. [b] Reference 11; uncertainties are ±15 ppm in principal components and ±30 ppm in anisotropies.

TABLE III: Carbon-13 Spin–Lattice Relaxation Times for Some Solid Metal Carbonyl Clusters[a]

compound	site	T_1,[b] s
$Os_3(CO)_{12}$	axial	413
	equatorial	432
$Rh_6(CO)_{16}$	terminal	520
	bridging	880
$Fe_3(CO)_{12}$	all	96

[a] Measured at room temperature at 38 MHz, using the saturating comb saturation-recovery method. [b] Estimated uncertainty ±10%.

of the chemical shift tensor for each site. However, close inspection of this spectrum reveals that the fine structure evident in the centerbands is repeated exactly in each sideband, indicating that all six axial carbonyl sites and all six equatorial sites have identical chemical shift anisotropies and asymmetry parameters. Observation of similar behavior in other metal carbonyl clusters (vide infra) indicates that sites that are different due only to crystallographic inequivalence, as opposed to those that are inequivalent in solution, have virtually identical CSA parameters. We list in Table II the principal components of the chemical shift tensor for one representative axial site and one equatorial site for $Os_3(CO)_{12}$. The CSA parameters for the two sites are very similar, both having small asymmetry parameters and anisotropies of ca. 370 ppm. Although these anisotropies are 5% higher than the 347-ppm value obtained from a broad-line spectrum,[11] the agreement is quite reasonable considering that only a single component was used to fit the latter.

We have also measured the spin–lattice relaxation times (T_1) for the carbonyl sites of $Os_3(CO)_{12}$ at 38 MHz, using the saturating comb saturation-recovery method.[22] We find T_1 values of ca. 420 s for both axial and equatorial sites, as listed in Table III. Such long ^{13}C relaxation times are common for nonfluxional binary metal carbonyls,[6,11] where there are no efficient pathways for spin–lattice relaxation. Carbon-13 T_1's are much shorter for metal carbonyl complexes containing protons, because ^1H–^{13}C dipolar coupling provides a relatively efficient relaxation mechanism. For example, we find a T_1 of ca. 10 s for the closely related osmium cluster $H_2Os_3(CO)_{10}$ and similar values for a variety of clusters of the form $HOs_3(CO)_{10}(OR)$.

$Ru_3(CO)_{12}$. As shown in Figure 2, we observe very similar ^{13}C MAS NMR spectra for $Ru_3(CO)_{12}$ (enriched to 74% in ^{13}C), which is isostructural with $Os_3(CO)_{12}$.[29] As with $Os_3(CO)_{12}$, two sets of centerband resonances are observed, attributable to axial and equatorial carbonyl sites. Both are split into six resonances

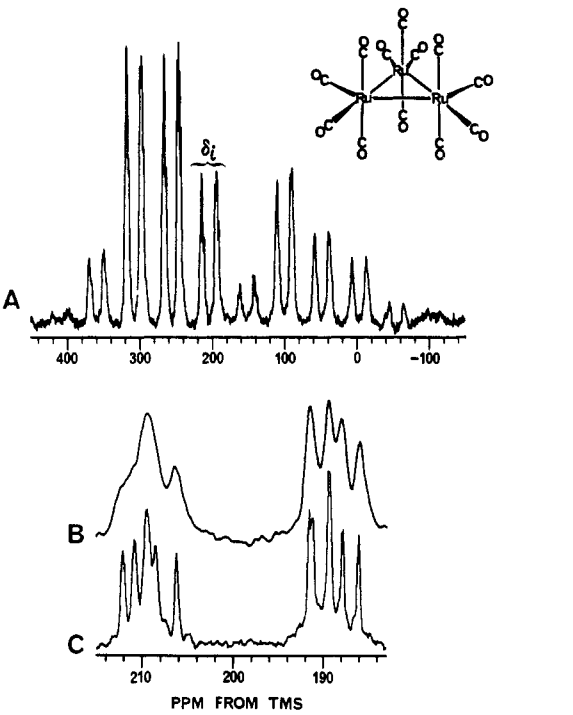

Figure 2. Carbon-13 MAS NMR spectra of $[^{13}C]Ru_3(CO)_{12}$. (A) Spectrum obtained at 38 MHz; 2.0-kHz spinning speed, 96 acquisitions with a 200-s recycle delay. (B) Expanded view showing centerband fine structure. (C) Expanded view of centerband resonances from a spectrum obtained at 90 MHz; 2.9-kHz spinning speed, 100 acquisitions with a 150-s recycle delay.

as a result of crystallographic inequivalence, producing a pattern very similar to that of $Os_3(CO)_{12}$. Again, we observe that the high-frequency group of resonances is significantly broader than the low-frequency group, consistent with unresolved $^2J_{CC}$(trans) coupling, allowing assignment of the high-frequency resonances to the axial carbonyls. It is interesting to note that this is the first time that separate resonances have been observed for $Ru_3(CO)_{12}$, since this cluster exhibits rapid axial–equatorial exchange in solution, down to the lowest attainable temperatures.[23] The average of the 12 resonances observed in the solid state (199.4 ppm) is very close to the exchange-averaged value measured in solution (199.7 ppm).[24]

We list in Table II the principal components of the chemical shift tensor for one axial and one equatorial carbonyl resonance of $Ru_3(CO)_{12}$. As with $Os_3(CO)_{12}$, the CSA parameters of the six axial and six equatorial resonances appear to be identical. The anisotropies we calculate for the two sites of $Ru_3(CO)_{12}$ are in good agreement with the broad-line results of Gleeson and Vaughan,[11] despite the fact that they analyzed their spectrum as arising from a single site. In contrast to the static results, however, we find that the chemical shift tensor asymmetry parameters of the carbonyls in this cluster are not significantly larger than zero. It is likely that the apparent axial asymmetry of the static line shape oserved for $Ru_3(CO)_{12}$ (η = 0.11)[11] is actually due to the overlap of two axially symmetric powder patterns, from the axial and equatorial carbonyls.

$Rh_6(CO)_{16}$. We shown in Figure 3A the ^{13}C MAS NMR spectrum of 40% ^{13}C-enriched $Rh_6(CO)_{16}$ obtained at 38 MHz. In solution, $Rh_6(CO)_{16}$ possesses O_h symmetry and yields a ^{13}C NMR spectrum with two resonances in a 3:1 ratio. These resonances are attributed to the terminal and triply bridging (μ_3) carbonyls, respectively.[30] The chemical shifts of the two resonances differ by 50 ppm, and thus they are readily resolved in the MAS spectrum. The chemical shift anisotropy of the terminal sites is similar to that of the terminal carbonyls in $Os_3(CO)_{12}$, ca. 400 ppm. However, the bridging carbonyl sites

(29) Churchill, M. R.; Hollander, F. J.; Hutchinson, J. P. *Inorg. Chem.* **1977**, *16*, 2655.

(30) Heaton, B. T.; Towl, A. D. C.; Chini, P.; Fumagalli, A.; McCaffrey, D. J. A.; Martinengo, S. *J. Chem. Soc., Chem. Commun.* **1975**, 523.

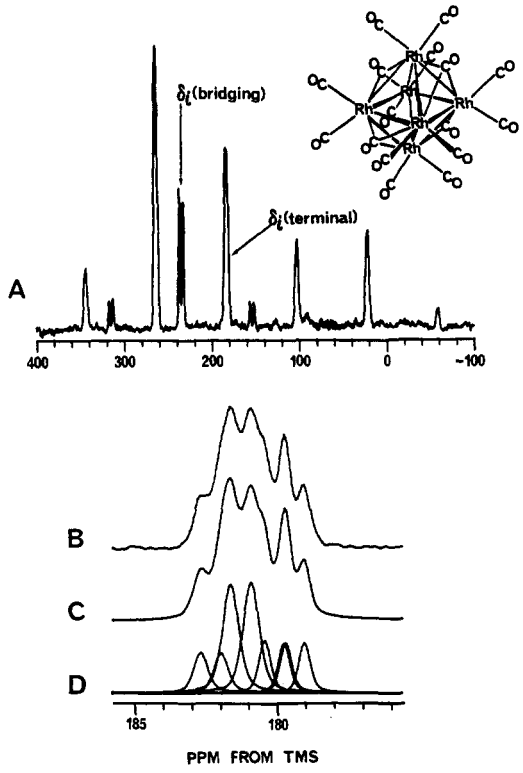

Figure 3. Carbon-13 MAS NMR spectra of $[^{13}C]Rh_6(CO)_{16}$. (A) Spectrum obtained at 38 MHz; 3.1-kHz spinning speed, 64 acquisitions with a 900-s recycle delay. (B) Expanded view of terminal carbonyl centerband region from a spectrum obtained at 90 MHz; 3.1-kHz spinning speed, 104 acquisitions with a 500-s recycle delay. (C, D) Simulation of (B) using four sets of doublets (J = 70 Hz) in a 1:3:1:1 ratio.

have an anisotropy of only 200 ppm[11] and thus yield relatively weak spinning sidebands at this field strength/spinning speed combination. Because of this large difference in chemical shift anisotropies, an accurate determination of the relative intensities of the two sites requires that the integrals be summed over all spinning sidebands for each site. From the spectrum of Figure 3A, we obtain a terminal/bridging ratio of 3.4:1, in reasonable agreement with the expected value of 3:1.

Despite the O_h point symmetry of $Rh_6(CO)_{16}$ in solution, the symmetry of the molecular units in the crystalline solid state is only C_2.[31] Thus, we expect two distinct resonances from the bridging carbonyls and six from the terminal sites. The splitting of the bridging carbonyl resonance can be seen in Figure 3A, since it is relatively large (4.3 ppm). However, the terminal carbonyl resonance at this field strength has a very complex shape (see Figure 4). At 90 MHz, however, the line shape can be simulated as shown in Figure 3B, using four sets of doublets (J = 70 Hz) with a relative intensity ratio of 1:1:3:1. The most intense doublet apparently arises from overlap of three sets of doublets. The splitting is due to J coupling to ^{103}Rh, which is 100% abundant and has $I = {}^1/_2$. In solution, the terminal carbonyl resonance is a doublet ($^1J_{RhC}$ = 70 Hz), while the bridging carbonyl resonance is split into a quartet ($^1J_{RhC}$ = 25 Hz) from coupling to three Rh atoms.[30] Our analysis of the terminal carbonyl resonance is supported by the observation that our simulation parameters correctly predict the observed line shapes at three different field strengths, as shown in Figure 4. The 25-Hz splitting of the bridging carbonyl resonances is apparently too small to observe, although we note that these resonances are significantly broader than those of the terminal carbonyls (75 Hz vs. 50 Hz at 90 MHz), consistent with an unresolved 1:3:3:1 quartet with J = 25 Hz.

We list in Table II our values for the principal components of the chemical shift tensor for one of the bridging carbonyl resonances of $Rh_6(CO)_{16}$ and for all of the terminal carbonyl resonances, the latter obtained by using the intensity integrated over the entire terminal carbonyl region. Because of the small number of sidebands observed for the bridging sites at 38 MHz, the CSA parameters for these sites were obtained from a 90-MHz spectrum, where many sidebands are observed. Our results are in excellent agreement with those of Gleeson and Vaughan,[11] who were able to obtain CSA parameters for both bridging and terminal carbonyl sites by broad-line NMR, because of the large difference in their anisotropies.

(31) Corey, E. R.; Dahl, L. F.; Beck, W. *J. Am. Chem. Soc.* **1963**, *85*, 1202.

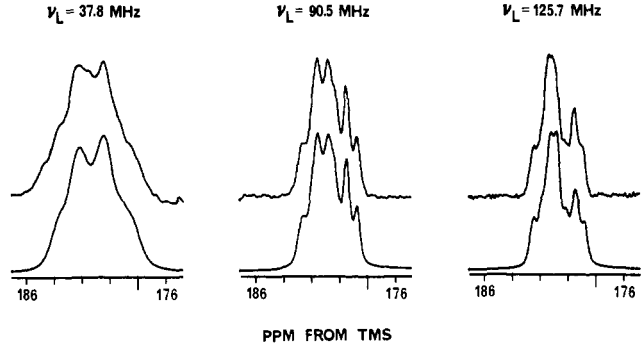

Figure 4. Expanded views of terminal carbonyl centerband resonances for $[^{13}C]Rh_6(CO)_{16}$ at three field strengths (top), along with simulations using identical parameters (bottom).

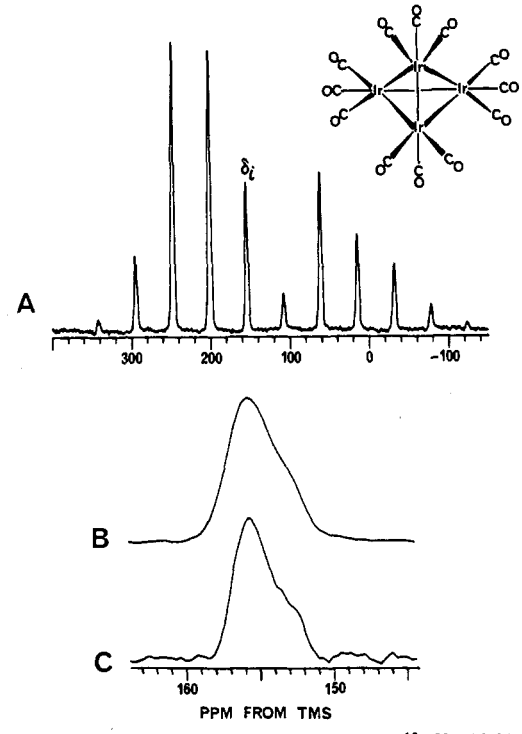

Figure 5. Carbon-13 MAS NMR spectra of $[^{13}C]Ir_4(CO)_{12}$. (A) Spectrum obtained at 90 MHz; 4.0-kHz spinning speed, 100 acquisitions with a 60-s recycle delay. (B) Expanded view of centerband resonance. (C) Expanded view of centerband region from a spectrum obtained at 125 MHz; 6.4-kHz spinning speed, 384 acquisitions with a 60-s recycle delay.

We have also measured ^{13}C spin–lattice relaxation times for $Rh_6(CO)_{16}$, as listed in Table III. As for $Os_3(CO)_{12}$, the T_1's for $Rh_6(CO)_{16}$ are several hundreds of seconds at 38 MHz. We find that the bridging carbonyl sites have a T_1 that is significantly longer than that of the terminal carbonyl sites. It is interesting to note that the ratio of the relaxation rates ($1/T_1$) for the two sites ($R_{terminal}/R_{bridging}$ = 1.7) is close to the ratio of their chemical shift anisotropies ($\Delta\delta_{terminal}/\Delta\delta_{bridging}$ = 1.9), which suggests that the larger T_1 of the bridging carbonyls may be at least partly attributable to their smaller chemical shift anisotropy.

$Ir_4(CO)_{12}$. We show in Figure 5A the ^{13}C MAS NMR spectrum of $[^{13}C]Ir_4(CO)_{12}$, obtained at 90 MHz. In solution, $Ir_4(CO)_{12}$ has T_d symmetry and thus yields a single ^{13}C resonance.

The chemical shift has been reported to be 154.2 ppm in chlorobenzene at 100 °C,[32] the high temperature being necessary because of the poor solubility of this cluster. The unit cell of crystalline $Ir_4(CO)_{12}$ contains three distinct molecules, each with C_3 symmetry, yielding 12 distinct carbonyl sites.[33] Experimentally, as shown in Figure 5B, we observe only a single broad resonance (ca. 400-Hz fwhh), centered at 156 ppm for this cluster. The resolution is not significantly improved at 125 MHz, as shown in Figure 5C. We believe this poor resolution is due to dipolar coupling between ^{13}C and the quadrupolar nuclides ^{191}Ir (37.3% abundant, $I = {}^3/_2$) and ^{193}Ir (62.7% abundant, $I = {}^3/_2$). Although magic-angle spinning generally eliminates dipolar couplings, coupling to quadrupolar nuclei is only partially averaged, due to quadrupolar perturbation of the Zeeman states. This effect is well-known in ^{13}C MAS studies of organic compounds, where it is commonly observed that carbon atoms adjacent to a nitrogen are broadened by incompletely averaged dipolar coupling to ^{14}N (99.6% abundant, $I = 1$).[34-37] The theory of this effect has been described by Zumbulyadis et al.[37] The extent of the broadening is governed by the ratio of the Larmor frequency (ν_L) of the quadrupolar nucleus to its quadrupole coupling constant (e^2qQ/h), the effect being most severe when ν_L is not much greater than e^2qQ/h. While most of the transition metals have quadrupolar isotopes, this effect will only be significant when the isotopes are abundant and have large quadrupole moments and/or small gyromagnetic ratios. On the basis of these critieria, this effect should be most prominent for Ir, Ta, Re, and Au and of less importance for Co, Mn, Cu, and Nb. It has been observed that rhenium carbonyl complexes such as $Re_2(CO)_{10}$ do indeed give severely broadened ^{13}C MAS NMR spectra,[38] and previously reported spectra of $Co_2(CO)_8$[8] and $Co_4(CO)_{12}$[10] also show abnormally broad resonances, although in the latter cases the situation is complicated by carbonyl exchange. It is important to note that this effect depends on the quadrupole coupling constant of the quadrupolar nucleus, which is the product of two terms: the nuclear quadrupole moment and the electric field gradient. Thus, it is strongly dependent on the symmetry of the metal sites, which affects the electric field gradients. For any metal site with tetrahedral or higher symmetry, the electric field gradient must be zero, and consequently no broadening should be seen.

The principal components of the shielding tensor for $Ir_4(CO)_{12}$ are listed in Table II. Our results are in agreement with the broad-line results of Gleeson and Vaughan,[11] with the exception of δ_{33}. However, the isotropic chemical shift calculated by these workers (167 ppm) is too high by ca. 12 ppm. Since δ_{11} and δ_{22} are generally obtained quite accurately from powder spectra, this most likely indicates that their δ_{33} value is too high by $3 \times 12 = 36$ ppm. Using Gleeson and Vaughan's δ_{11} and δ_{22} values and the correct δ_i value of 156 ppm gives $\delta_{33} = -86$ ppm, in good agreement with our value of −81 ppm.

$Fe_3(CO)_{12}$. We show in Figure 6A the ^{13}C MAS NMR spectrum of 35% ^{13}C-enriched $Fe_3(CO)_{12}$ obtained at 90 MHz. As shown by Wei and Dahl,[39] in the solid state $Fe_3(CO)_{12}$ has the C_{2v} structure shown in Figure 6, with two carbonyls bridging one of the Fe–Fe bonds. However, the solid exhibits an inversion disorder, with the two orientations of Figure 7 occurring with equal probability. As shown by Dorn et al.,[7,9] these two orientations can be interconverted by a 60° rotation of the Fe_3 triangle, with the carbonyl ligands remaining fixed in the crystal lattice. Although this rotation is slow on the X-ray diffraction time scale, it is fast on the NMR time scale at room temperature, so that

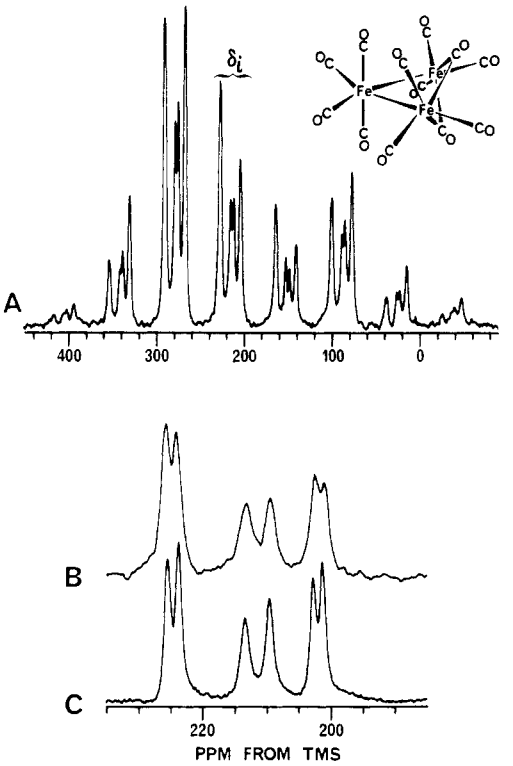

Figure 6. Carbon-13 MAS NMR spectra of $[^{13}C]Fe_3(CO)_{12}$. (A) Spectrum obtained at 38 MHz; 2.4-kHz spinning speed, 16 acquisitions with a 900-s recycle time. (B) Expanded view of centerband resonance. (C) Expanded view of centerband obtained at 90 MHz; 3.1-kHz spinning speed, 148 acquisitions with a 30-s recycle time.

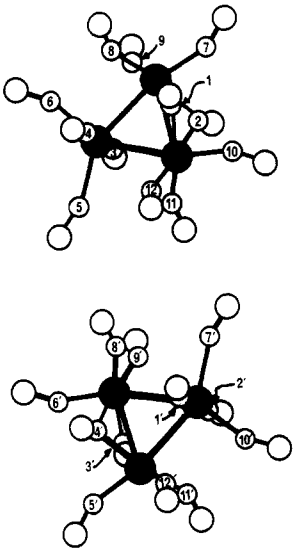

Figure 7. Structure of $Fe_3(CO)_{12}$ showing the interconverting enantiomers. The filled circles are Fe atoms, the open circles O atoms, and the numbered circles C atoms.

an averaged spectrum is obtained with only six distinct carbon resonances being observed.[7] This motion results in each carbonyl ligand alternating between two different bonding arrangements with respect to the Fe_3 triangle, although there is only slight movement of the carbonyls themselves. Since the two orientations of Figure 7 are related by an inversion center, C1 and C3′, C2 and C4′, etc., are equivalent. Thus, the exchanging pairs are C1 and C3, C2 and C4, C5 and C7, C6 and C10, C8 and C11, and C9 and C12, using the numbering system of Cotton and Troup.[40]

As shown in Figure 6, we observe six centerband resonances for $Fe_3(CO)_{12}$, with chemical shifts in good agreement with those of Dorn et al.[7] It can be seen that, despite the rapid motion of

(32) Stuntz, G. F. Ph.D. Thesis, University of Illinois at Urbana—Champaign, 1974; p 300.
(33) Churchill, M. R.; Hutchinson, J. P. *Inorg. Chem.* **1978**, *17*, 3528.
(34) Frey, M. H.; Opella, S. J. *J. Chem. Soc., Chem. Commun.* **1980**, 474.
(35) Groombridge, C. J.; Harris, R. K.; Packer, K. J.; Say, B. J.; Tanner, S. F. *J. Chem. Soc., Chem. Commun.* **1980**, 174.
(36) Naito, A.; Ganapathy, S.; McDowell, C. A. *J. Chem. Phys.* **1981**, *74*, 5393.
(37) Zumbulyadis, N.; Henrichs, P. M.; Young, R. H. *J. Chem. Phys.* **1981**, *75*, 1603.
(38) Henly, T.; Shapley, J. R., private communication.
(39) Wei, C. H.; Dahl, L. F. *J. Am. Chem. Soc.* **1969**, *91*, 1351.
(40) Cotton, F. A.; Troup, J. M. *J. Am. Chem. Soc.* **1974**, *96*, 4155.

TABLE IV: Calculated Exchange-Averaged Chemical Shift Tensor Components, Anisotropies, and Asymmetry Parameters for $Fe_3(CO)_{12}$

sites	ϕ, deg	δ'_{11}, ppm	δ'_{22}, ppm	δ'_{33}, ppm	$\Delta\delta'$, ppm	η
C1/C3	13.5	322	319	35	285	0.02
C2/C4	21.0	322	315	40	279	0.04
C5/C7	14.9	354	347	−78	428	0.03
C6/C10	38.1	354	307	−38	369	0.19
C8/C11	49.2	354	278	−9	325	0.35
C9/C12	32.7	354	319	−50	387	0.13

the Fe_3 triangle, the chemical shift anisotropy of the carbonyls is largely retained, as previously noted.[11] In contrast to the broad-line results of Gleeson and Vaughan, however, our MAS results allow CSA parameters to be obtained for each site, as listed in Table II. We can clearly discern differences between the sites, with the highest frequency pair of resonances having the smallest anisotropies. These resonances arise from the two pairs of exchanging sites involving bridging carbonyls, i.e., C1 and C3 and C2 and C4. The small anisotropies are the result of averaging the ca. 450-ppm anisotropy of a terminal carbonyl with the ca. 150-ppm anisotropy of a μ_2-carbonyl, yielding a resultant anisotropy of approximately 300 ppm.

It is a straightforward matter to calculate the exchange-averaged shielding tensors from the rigid-lattice tensors of the exchanging carbonyls, using a two-site exchange model.[41] We assume that the rigid-lattice tensors are axially symmetric, with the unique direction aligned along the C–O bond axis. Although there is little motion of the carbonyl ligands accompanying the movement of the Fe_3 triangle, the two orientations of each carbonyl site do not overlap exactly.[40] We thus need to know the angle ϕ formed by the C–O bond vectors of the two interchanging orientations of each site, which can be readily calculated from the structure refinement of Cotton and Troup.[40] Designating the rigid-lattice principal components of the two exchanging sites, labeled A and B, as $^A\delta_\perp$, $^A\delta_\parallel$ and $^B\delta_\perp$, $^B\delta_\parallel$, the exchange-averaged tensor is given by

$$\tilde{\delta}' = \tfrac{1}{2}({}^A\tilde{\delta} + {}^B\tilde{\delta}) = \begin{pmatrix} \delta'_{xx} & \delta'_{xy} & 0 \\ \delta'_{xy} & \delta'_{yy} & 0 \\ 0 & 0 & \delta'_{zz} \end{pmatrix}$$

where

$$\delta'_{xx} = \tfrac{1}{2}({}^A\delta_\parallel + {}^B\delta_\parallel \cos^2\phi + {}^B\delta_\perp \sin^2\phi)$$

$$\delta'_{xy} = \tfrac{1}{2}(\cos\phi \sin\phi)({}^B\delta_\perp - {}^B\delta_\parallel)$$

$$\delta'_{yy} = \tfrac{1}{2}({}^A\delta_\perp + {}^B\delta_\parallel \sin^2\phi + {}^B\delta_\perp \cos^2\phi)$$

$$\delta'_{zz} = \tfrac{1}{2}({}^A\delta_\perp + {}^B\delta_\perp)$$

After diagonalization, the principal components of the exchange-averaged tensor, designed δ'_{11}, δ'_{22}, and δ'_{33}, are obtained. Since we have been unable to measure the rigid-lattice principal components for $Fe_3(CO)_{12}$, which requires a low-temperature MAS spectrum, we have instead used the values measured for $(\eta^5\text{-}C_5H_5)Fe_2(CO)_4$: $\Delta\delta_{terminal}$ = 440 ppm, η = 0 and $\Delta\delta_{bridging}$ = 140 ppm, η = 0.[11] The results based on these values are given in Table IV. In general, the exchange-averaged tensors are not axially symmetric, despite the assumption of axial symmetry for the rigid-lattice tensors. The asymmetry parameter is determined by the angle ϕ, with axial symmetry occurring only for $\phi = n(\pi/2)$ (n = 0, 1, 2, ...). Considering the uncertainty arising from the use of the rigid-lattice CSA of a different compound, the agreement is quite good. For the exchanging pairs C1/C3 and C2/C4, we calculate anisotropies of ca. 280 ppm and small asymmetry parameters, in agreement with the values measured for the resonances at 225.5 and 223.8 ppm (obtained by integration over both): $\Delta\delta$ = 298 ppm, η = 0.04. Although the assignment of the other resonances is not as straightforward, there appears to be a close correspondence between the calculated CSA parameters for C8/C11 and the 213.5-ppm resonance (calculated: $\Delta\delta'$ = 325 ppm, η = 0.35; found: $\Delta\delta'$ = 350 ppm, η = 0.16) and C9/C12 and the 209.7-ppm resonance (calculated: $\Delta\delta'$ = 387 ppm, η = 0.13; found: $\Delta\delta'$ = 378 ppm, η = 0.06). This leaves the pairs C5/C7 and C6/C10 to be assigned to the resonances at 202.9 and 201.4 ppm. Although our calculations indicate that there should be significant differences between these two resonances, we are unable to obtain separate CSA parameters because of the overlap between them. We note, however, that the average values of the calculated CSA parameters of the C5/C7 and C6/C10 pairs ($\Delta\delta'_{av}$ = 398 ppm, η'_{av} = 0.11) are in close agreement with those obtained for the 202.9- and 201.4-ppm resonances (obtained by integration over both): $\Delta\delta$ = 386 ppm, η = 0.08.

The spin–lattice relaxation times measured for $Fe_3(CO)_{12}$ at 38 MHz are listed in Table III. For all three pairs of resonances we find T_1's of ca. 96 s, in agreement with the value of 80 s reported by Hanson[6] at 15 MHz. The faster relaxation of the carbonyls in $Fe_3(CO)_{12}$ relative to those of the other clusters is a result of the motion of the Fe_3 framework. The displacements of the carbonyl ligands caused by rotation of the iron triangle, although small, are large relative to the normal thermal displacements in nonfluxional clusters. These larger angular fluctuations, in conjunction with the large ^{13}C chemical shift anisotropy, result in more efficient spin–lattice relaxation.

Conclusions

The results presented above indicate, we believe, the utility of high field ^{13}C MAS NMR experiments for studying metal carbonyl clusters in the crystalline solid state. With the 0.25-ppm resolution obtainable at 90 MHz, it is often possible to distinguish all crystallographically inequivalent sites, yielding information on solid-state symmetry. There are several factors that affect the resolution obtained in these experiments. As demonstrated for $Ir_4(CO)_{12}$, resonances from carbonyls bound to metals that have abundant quadrupolar isotopes may be severely broadened due to incompletely averaged dipolar coupling between ^{13}C and the quadrupolar isotopes. The level of ^{13}C enrichment is also clearly important, since broadening from ^{13}C–^{13}C J coupling begins to be significant at levels approaching 40–50%. In general, we have used enrichment levels that are higher than this in order to achieve greater sensitivity in examining these clusters when supported on metal oxides.[3] In some cases, we have observed narrower line widths at lower enrichment levels, as with the axial carbonyl resonances of $Os_3(CO)_{12}$ and $Ru_3(CO)_{12}$. However, when the J coupling is small, as for the equatorial carbonyl resonances of these clusters, little improvement in the line widths is observed at low enrichment levels.

Another important factor affecting resolution is the magnetic field strength. As demonstrated above, we consistently observe improvements in resolution as the field strength is increased. Some of this improvement is due to the decreased importance of J coupling relative to chemical shifts at higher magnetic field strengths. However, even for resonances that do not appear to be appreciably broadened by J coupling, we find significantly narrower line widths (in ppm) at high field. At very high field strengths (90 MHz and above), however, setting of the magic angle becomes critical. The broadening caused by a 1° deviation from the magic angle is approximately 2.5% of the static line width.[42] Assuming an anisotropy of 400 ppm, a typical static line width at 90 MHz is 36 kHz. Thus, an 0.1° error in the spinning angle should introduce an additional 90 Hz to the line width. However, using the method of Frye and Maciel,[21] which allows the magic angle to be set to within ±0.05°, we find that line widths of 25 Hz or less can consistently be obtained at 90 MHz.

In addition to high-resolution information, we have also shown that accurate chemical shift anisotropy parameters can be obtained from slow MAS spectra, our values being in good agreement with the earlier broad-line results of Gleeson and Vaughan.[11] The only cases where there are significant discrepancies between our results

(41) Spiess, H. W. *Chem. Phys.* **1974**, *6*, 217.

(42) Andrew, E. R. *Proc. Nucl. Magn. Reson. Spectrosc.* **1971**, *8*, 1.

and those of Gleeson and Vaughan are for $Ir_4(CO)_{12}$ and $Fe_3(CO)_{12}$. As described above, the discrepancy for $Ir_4(CO)_{12}$ is most likely due to an inaccurate determination of δ_{33} in the broad-line results, this value being generally difficult to measure accurately at low signal-to-noise levels. For $Fe_3(CO)_{12}$, the overlap of six powder patterns with different CSA parameters produces a powder line shape that is particularly difficult to deconvolute. However, the CSA parameters for each site can be readily obtained from slow MAS spectra, allowing comparison of the experimental values with those calculated for a two-site exchange model. Slow-spinning MAS experiments should prove to be a valuable addition to fast-spinning MAS experiments in elucidating more complex exchange processes such as those occurring in $Co_2(CO)_8$[8] and $Co_4(CO)_{12}$.[10]

Note Added in Proof. After submission of the article, results of similar experiments on $Os_3(CO)_{12}$ and $Ru_3(CO)_{12}$ were reported.[43] These results are in good agreement with those presented above.

Acknowledgment. This work was supported in part by the U.S. National Science Foundation Solid-State Chemistry Program (Grant DMR 86-15206).

Registry No. $[^{13}C]Fe_3(CO)_{12}$, 117678-70-3; $[^{13}C]Ru_3(CO)_{12}$, 117678-71-4; $[^{13}C]Os_3(CO)_{12}$, 112426-48-9; $[^{13}C]Rh_6(CO)_{16}$, 117733-83-2; $[^{13}C]Ir_4(CO)_{12}$, 117678-68-9.

(43) Aime, S.; Botta, M.; Gobetter, R.; Osella, D.; Milone, L. *Inorg. Chim. Acta* **1988**, *146*, 151.

Molecular Structure of Gaseous 1,2-Dibromocyclobutene-3,4-dione ($C_4O_2Br_2$) As Determined by Electron Diffraction

Kolbjørn Hagen*

Department of Chemistry, University of Trondheim, AVH, N-7055 Trondheim, Norway

and Bruno Lunelli

Università di Bologna, Dipartimento Chimico "G. Ciamician", 2 via Selmi, and Istituto di Spettroscpia Molecolare CNR, 1 via de Castagnoli, I-40126 Bologna, Italy *(Received: July 15, 1988)*

The structure of 1,2-dibromocyclobutene-3,4-dione at 77 °C has been investigated by gas-phase electron diffraction. The experimental data comply with a planar molecule of C_{2v} point group symmetry. Values of the bond distances (r_g) and valence angles ($\angle_\alpha$) with estimated 2σ uncertainties are r(C=O) = 1.185 (4), r(C=C) = 1.356 (14), $r(C_{Br}—C_O)$ = 1.518 (10), $r(C_O—C_O)$ = 1.589 (18), r(C—Br) = 1.831 (4) Å, ∠C=C—C = 94.4 (4), ∠C—C—C = 85.6 (4), ∠C=C—Br = 133.0 (5), $\angle C_O—C—Br$ = 132.6 (7), $\angle C_O—C=O$ = 139.4 (18), and $\angle C_{Br}—C=O$ = 135.0 (20)°.

Introduction

Because of interest in the features and dynamics of species containing cyclobutenedione moieties,[1] we have recently determined bond distances, valence angles, and vibrational amplitudes in 1,2-dichlorocyclobutene-3,4-dione (CCB) using gas-phase electron diffraction.[2] This investigation was also part of a research program on the structure of molecules with rings in which the conjugated chain O=C—C=C—C=O exists.[3-7] We have also been able to synthesize the bromine analogue of CCB, 1,2-dibromocyclobutene-3,4-dione (hereafter BCB), Figure 1, and the results of a spectroscopic investigation of these molecules have been published.[8] Since BCB is a new molecule whose structure has not been determined earlier, we thought it worthwhile to investigate the sensitivity of the cyclobutene-3,4-dione structure to the substitution of the two chlorine atoms with the larger and more polarizable, but less electronegative bromine atoms. We have therefore carried out an electron diffraction investigation of gaseous BCB, the results of which are the object of this article.

Experimental Section and Data Reduction

BCB was prepared and purified as reported earlier.[8] Electron diffraction photographs were recorded at 77 °C with a Balzers Eldigraph KDG-2[9,10] on Kodak electron image plates. The electron wavelength was calibrated against benzene,[11] and optical densities were measured with a Joyce Loebl microdensitometer. Five plates from the long (496.93 mm) and four from the short (248.13 mm) nozzle-to-plate distance experiments were selected for analysis. The data were reduced in the usual way,[12-14] and a calculated background[15] was subtracted from the data for each plate to yield experimental molecular intensity curves in the form $sI_m(s)$. The average experimental intensity curves are shown in Figure 2. The ranges of intensity data were $2.00 \le s/Å^{-1} \le 14.50$ and $4.00 \le s/Å^{-1} \le 26.00$, and the data interval was $\Delta s = 0.25$ $Å^{-1}$. The intensity and background data are available as supplementary material (see paragraph at end of text). Radial distribution (RD) curves (Figure 3) were calculated by Fourier transforming the function $I'(s) = sI_m(s)Z_CZ_{Br}A_C^{-1}A_{Br}^{-1}\exp(-Bs^2)$ with $B = 0.0020$ Å^2. Electron scattering amplitudes ($f = A/s^2$) and phases (η) for all calculations were taken from tables.[16]

Structure Analysis

The radial distribution curve for BCB is consistent with point group C_{2v}, the same as that for the chlorine analogue. The geometry of BCB can be defined uniquely by seven independent

(1) Lunelli, B.; Busetti, V. *J. Mol. Struct.* **1987**, *160*, 287.
(2) Hagen, K.; Hedberg, K.; Lunelli, B.; Giorgini, M. G. *J. Phys. Chem.* **1988**, *92*, 4313.
(3) Hagen, K.; Hedberg, K. *J. Mol. Struct.* **1978**, *44*, 195.
(4) Hagen, K.; Hedberg, K. *J. Mol. Struct.* **1978**, *50*, 103.
(5) Hagen, K.; Hedberg, K. *J. Chem. Phys.* **1973**, *59*, 158.
(6) Hagen, K.; Hedberg, K. *J. Mol. Struct.* **1978**, *49*, 351.
(7) Schei, H.; Hagen, K.; Traetteberg, M.; Seip, R. *J. Mol. Struct.* **1980**, *62*, 121.
(8) Lunelli, B.; Giorgini, M. G. *Spectrochim. Acta* **1987**, *43A*, 829.
(9) Zeil, W.; Haase, J.; Wegmann, L. *Z. Instrumentenkd.* **1966**, *74*, 84.
(10) Bastiansen, O.; Graber, R.; Wegmann, L. *Balzers High Vac. Rep.* **1969**, *25*, 1.
(11) Tamagawa, K.; Iijima, T.; Kimura, M. *J. Mol. Struct.* **1976**, *30*, 243.
(12) Hagen, K.; Hedberg, K. *J. Am. Chem. Soc.* **1973**, *95*, 1003.
(13) Gundersen, G.; Hedberg, K. *J. Chem. Soc.* **1969**, *51*, 2500.
(14) Andersen, B.; Seip, H. M.; Strand, T. G.; Stølevik, R. *Acta Chem. Scand.* **1969**, *23*, 3224.
(15) Hedberg, L. *Abstracts of the Fifth Austin Symposium on Gas Phase Molecular Structure*, Austin, TX, March, 1974; p 37.
(16) Schäfer, L.; Yates, A. C.; Bonham, R. A. *J. Chem. Phys.* **1971**, *56*, 3056.

0022-3654/89/2093-1326$01.50/0